Published in final edited form as:
*Curr Biol*. 2006 June 20; 16(12): 1217–1223. doi:10.1016/j.cub.2006.04.046.

# Kinetochores Use a Novel Mechanism for Coordinating the Dynamics of Individual Microtubules

**Kristin J. VandenBeldt**[1], **Rita M. Barnard**[1], **Polla J. Hergert**[1], **Xing Meng**[1], **Helder Maiato**[2,3], and **Bruce F. McEwen**[1,4,*]

[1] Wadsworth Center, New York State Department of Health, Albany, New York 12201

[2] Institute for Molecular Cell Biology, Rua do Campo Alegre, 823, 4150-180 Porto, Portugal

[3] Laboratory of Molecular and Cell Biology, Faculdade de Medicine, University Porto, 4050-345 Porto, Portugal

[4] Department Biomedical Sciences, School of Public Health, State University of New York at Albany, Albany, New York 12222

## Summary

Chromosome alignment during mitosis is frequently accompanied by a dynamic switching between elongation and shortening of kinetochore fibers (K-fibers) that connect kinetochores and spindle poles [1,2]. In higher eukaryotes, mature K-fibers consist of 10–30 kinetochore microtubules (kMTs) whose plus ends are embedded in the kinetochore [1–3]. A critical and long-standing question is how the dynamics of individual kMTs within the K-fiber are coordinated [1–5]. We have addressed this question by using electron tomography to determine the polymerization/depolymerization status of individual kMTs in the K-fibers of PtK1 and *Drosophila* S2 cells. Surprisingly, we find that the plus ends of two-thirds of kMTs are in a depolymerizing state, even when the K-fiber exhibits net tubulin incorporation at the plus end [6–8]. Furthermore, almost all individual K-fibers examined had a mixture of kMTs in the polymerizing and depolymerizing states. Therefore, although K-fibers elongate and shrink as a unit, the dynamics of individual kMTs within a K-fiber are not coordinated at any given moment. Our results suggest a novel control mechanism through which attachment to the kinetochore outer plate prevents shrinkage of kMTs. We discuss the ramifications of this new model on the regulation of chromosome movement and the stability of K-fibers.

## Results and Discussion

Cryo-electron microscopy studies of in vitro preparations have established that MT plus ends adopt a straight conformation (either as an open sheet or blunt end) during polymerization and a curved conformation during depolymerization [9–13]. We have used semi-automated electron tomography to determine the plus-end conformations of a large number of kMTs from $PtK_1$ and *Drosophila* S2 cells (Figures 1A–1C) [14–16]. Figures 1D and 1E illustrate the variety of plus-end conformations found in our analysis of over 400 kMTs. These conformations are similar to those reported for MTs assembled in vitro and kMTs from *C. elegans* spindles [9–12,17]. Similar conformations were also detected in MTs

*Correspondence: bruce.mcewen@wadsworth.org.

Supplemental Data

Supplemental Data include three figures, one table, and a description of the methods used, and are available with this article online at http://www.current-biology.com/cgi/content/full/16/12/1217/DC1/.

that were not attached to the kinetochore (Figure S1). Surprisingly, a substantial proportion of the straight kMT plus ends we observed were capped (Figure 1D, third panel). Similar capping structures were previously detected on the minus ends of *C. elegans* kMTs but not on the plus ends [17]. We have no data concerning the structure or composition of this apparent cap, and we do not know its effect on kMT growth.

Based upon the analysis of Janosi et al., we classified slightly flared conformations with the straight group (Figure 1D, fourth panel) [12]. In practice, however, we only observed a small number of kMT plus ends that fell into the slightly flared category. We classified kMT plus ends as curved when the ends of the kMT were curled around at least far enough to form a right angle to the body of the MT. The fourth panels in Figures 1D and 1E show the most highly flared kMT plus end of the straight group and the least curled kMT plus end of the curved group. The table in Figure S2 lists the number and percentage of kMT plus ends exhibiting each conformation type shown in Figures 1D and 1E.

We used the above scheme to classify the plus-end conformations of kMTs in metaphase, taxol-treated, nocodazole-treated, and anaphase $PtK_1$ cells. As can be seen from Figure 2, drug treatment dramatically altered the distribution of plus-end conformations, from 33% straight in control cells to 88% straight after taxol treatment, and to 6% straight after nocodazole treatment (see also Figure S2). These results are consistent with the known effects of micromolar levels of taxol and nocodazole to respectively promote MT polymerization and depolymerization [18]. Similarly, the shift in plus-end conformations to 7% straight after transition into anaphase is consistent with the predominately poleward movement of kinetochores during anaphase, a directionality that requires that K-fibers shorten from the plus end [1,6,7,19]. In summary, the kMTs we analyzed display plus-end conformations similar to those detected by cryo-electron microscopy in vitro preparations, and the ratio of straight to curved conformations shifts in the expected way with drug treatment or change of mitotic phase.

Nevertheless, a full analysis of the data in Figure 2 supports the surprising conclusion that plus-end conformations of kMTs are poorly correlated to net tubulin assembly or disassembly at the plus end of the K-fiber. During metaphase in $PtK_1$ cells, some, but not all, chromosomes oscillate around the spindle equator [19]. Thus, at any given moment in time, some kinetochores are moving toward their attached spindle pole with shortening K-fibers, others are moving away from the spindle pole with growing K-fibers, and still others are stationary with no change in K-fiber length. Because the data set of kMT plus ends in untreated metaphase cells comes from a large number of different kinetochores, kMTs from growing and shrinking K-fibers will roughly balance one another. Furthermore, a significant fraction of the kMTs in the metaphase data set comes from K-fibers that are neither growing nor shrinking. Hence, the profile of kMT conformations for the metaphase data set that is illustrated in Figure 2 represents a situation of no net change in K-fiber length. However, maintaining a constant K-fiber length requires net tubulin assembly at kMT plus ends in order to balance the constant tubulin disassembly at kMT minus ends [2,8]. This is clearly demonstrated by the observation that K-fibers steadily shorten from the minus end when both assembly and disassembly of kMT plus ends are inhibited by taxol treatment [20]. Therefore, the majority of kinetochore plus ends ought to exhibit the straight conformation during metaphase if there were a strong correlation between conformation and assembly state. Instead, we find that the majority (67%) of the kMT plus ends exhibit the curved conformation that is associated with disassembly (Figure 2).

We verified the preceding statistical argument by determining the plus-end conformations of kMTs in metaphase *Drosophila* S2 cells. S2 cells show a relatively fast flux rate during metaphase, but the chromosomes do not oscillate [21]. Consequently, all K-fibers

continuously exhibit net tubulin assembly at the plus ends. Therefore, most, if not all, of the plus ends of kMTs in metaphase S2 cells should be in the straight conformation [20,21]. Surprisingly, we again see a roughly 1:2 ratio of straight to curved plus-end conformations (Figure 2).

A caveat to the above conclusion is that although high-pressure freezing followed by freeze substitution provides better structural preservation than conventional procedures, there is the unlikely possibility that the very brief exposure to high pressure prior to freezing initiates transition to the disassembly phase in some kMTs [22]. To control for that possibility, we also prepared $PtK_1$ cells by room-temperature fixation with glutaraldehyde in a MT-stabilizing buffer. Although this is a slower, less optimal fixation procedure, it does avoid exposure to high pressure. The results for untreated and drug-treated metaphase cells were virtually the same as for high pressure frozen specimens (Figure S3). In summary, although the results are surprising, we find essentially the same pattern for two different cell types and two different fixation conditions.

The rapidity with which kinetochores can change their direction of movement implies that the growth states of kMTs in a given K-fiber are coordinated [1,19]. In order to test this idea, we compared plus-end conformations between individual kMTs bound to the same kinetochore, in untreated metaphase cells. As can be seen in Figure 3A, individual kMTs attached to the same kinetochore rarely exhibit complete uniformity of their plus-end conformations. On the other hand, if kMT conformations on individual kinetochores were totally uncoordinated, then the kMTs on most kinetochores would exhibit close to the 1:2 ratio of straight to curved conformations observed overall for kMTs in untreated metaphase cells (Figure 2). Instead, the graph in Figure 3A shows one kinetochore exhibiting a strong preference for the straight conformation and the other kinetochores exhibiting a range of ratios from 1:1 to all curved. We tested this further by plotting a histogram of the percentage of kMTs exhibiting the curved conformation in 27 kinetochores from untreated metaphase cells (Figure 3B). The histogram does not show a Gaussian distribution centered on 67% in the curved conformation as would be expected if kMT plus-end conformations were not influenced by the local kinetochore environment. Rather the data shows a broad distribution with a weak secondary peak at a low percent of curved ends and a primary peak at a percentage of curved plus ends that is higher than 67% (Figure 3B). These results indicate that although the conformations of MT plus ends on a given kinetochore are not tightly co-ordinated, individual kinetochores are generally biased toward a preponderance of kMTs in one of the two conformations.

We carried out a similar analysis on sister kinetochores in $PtK_1$ cells and found that some sister pairs are coordinated with each other, whereas others are not (Figure 3C). We also examined kMT plus-end conformations on six kinetochores in *Drosophila* S2 cells and found that four of the kinetochores had a mixture of kMT plus-end conformations (Figure 3D). These results are consistent with the notion that individual kinetochores can be biased toward growth or shrinkage and that sometimes sister kinetochores pull in opposite directions [19].

The data in Figure 3 indicate that kMT plus-end dynamics is not tightly coordinated in either S2 or $PtK_1$ cells. Although this contradicts the prevailing view of tight coordination between different kMTs of the same kinetochore, there are earlier studies indicating that kMTs in a single K-fiber do not have to be in the same growth state. For example, when biotin-labeled tubulin was injected into $PtK_1$ cells, some K-fibers only incorporated the label into a few of the kMTs [23]. Similarly, when biotin-labeled tubulin was injected into $PtK_1$ cells at early to mid anaphase, the label incorporated into K-fibers, even though most kinetochores are moving poleward [24]. This is consistent with our observation that even early anaphase cells

have some kMTs in the growing conformation (Figure 2). Thus, there is some precedent for microheterogeneity in the dynamic behavior of kMT plus ends in the same K-fiber. Although the minus-end disassembly of kMTs in fluxing systems is thought to proceed continuously, presumably the microheterogeneity we have detected at the plus end could be present at the minus end as well.

The data in Figures 2 and 3 reveal a surprisingly weak correlation between kMT dynamics and K-fiber growth. To further investigate the structural basis for this relationship, we determined the position of kMT plus ends in our data pool relative to the corona, outer plate, and heterochromatin (Figure 4A). Figure 4B illustrates that 86% of the kMTs in metaphase cells terminate in the outer plate, whereas only 9% penetrate into the heterochromatin and 5% terminate in the corona. Taxol does not stimulate a significant increase in the percentage of kMTs that penetrate into the heterochromatin, but nocodazole does completely inhibit penetration into the heterochromatin. These data are consistent with the hypothesis that molecules such as MCAK rapidly disassemble kMTs penetrating into the heterochromatin (Table S1) [25, 26]. Only a small percentage of the kMTs end in the corona, and we believe that these are likely to be in the process of association or disassociation. Previous studies have also found that most MTs terminate in the kinetochore outer plate [27]. However, the combination of electron tomography, optimal specimen preservation, and a large sample size enabled us to achieve greater precision in localizing the plus ends and quantifying the results.

The data in Figure 4B establish a remarkable feature of the kinetochore: the plus ends of almost all attached MTs are confined to a relatively narrow space defined by the outer plate. Therefore, it is highly probable that the outer plate is the site that mediates the attachment, plus-end conformation, and growth state of kMTs. The kinetochore outer plate is a fibrous network, and the termination of kMTs in the outer plate implies that the plus ends are enmeshed in this fibrous network [28]. We hypothesize that molecular components of the network inhibit MTs with curved plus ends from dissociating, which in turn prevents their rapid shrinkage. This hypothesis is consistent with the observation that kMTs in most cells are stable against a variety of disassembly agents and have a low turnover rate [29, 30]. The hypothesis is also supported by the frequent occurrence of distortions suggestive of constraint on the curved conformation (Figure 4C).

The results of our tomographic analysis call for a new way to look at the control of kMT dynamics. The model in Figure 5 postulates that during metaphase, kMT plus ends undergo catastrophe twice as often as rescue. However, kMTs in the disassembly phase do not necessarily disassemble because they are restrained by attachments to the outer plate. This restraint causes a local rise in tension around kMTs in the disassembly conformation, which stimulates their rescue [19,31,32]. In contrast, kMTs in the assembly conformation are under lower tension, which stimulates catastrophe. The net result is a robust cycle of dynamic instability that produces a continuous exchange of individual kMTs in the assembly conformation. Hence, the K-fiber as a whole exhibits a net incorporation of tubulin sub-units, even though at any one point in time only one-third of the kMTs are growing. The incomplete coordination of microtubule dynamics could partially explain the “governor” effect that refers to the observation that growth and shrinkage rates are slower for kMTs than for isolated MTs [1].

Although the model in Figure 5 predicts that kinetochores do not directly control the dynamics of individual kMTs, factors such as drugs can bias kMT dynamics on individual kinetochores toward the growing or shrinking conformations. For example, the data in Figure 2 can be explained by taxol treatment shifting the ratio between catastrophe and rescue rates toward rescue and nocodazole treatment shifting the ratio toward catastrophe. In

addition, factors such as tension and stage of mitosis can be seen as biasing the kinetochore to favor growth or shrinkage of kMT plus ends. Thus, transition into anaphase involves several regulatory changes that presumably act through the kinetochore outer plate to shift the ratio between kMT plus-end catastrophe and rescue rates toward catastrophe (Figure 2).

Expansion of the model in Figure 5 to include distinct states of the kinetochore also resolves the apparent contradiction between our data and the observation that the MT plus-end binding protein EB1 only binds to kinetochores when they are moving away from the attached spindle pole (i.e., EB1 only binds when the K-fiber is growing) [33]. Generally, this observation is interpreted to mean that EB1 has a strong preference for binding to the growing (straight) conformation of kMT plus ends. Our data is in conflict with this interpretation because EB1 binding to the kinetochore is an all or none effect, showing complete dissociation or association as the direction of motion is changed, while we observe a microheterogeneity of kMT plus-end conformations within individual K-fibers. However, EB1 binding data is also compatible with a model in which EB1 binds to kinetochore components that are coregulated with K-fiber growth or shrinkage [33]. This latter model predicts that the kinetochore is in different biochemical states during K-fiber growth and K-fiber shrinkage. When this model is combined with our kMT conformation data, we obtain a model in which the kinetochore as a whole has at least two distinct states: one state that supports K-fiber growth, EB1 binding, and biases individual kMT plus ends toward the growing (straight) conformation; and another state that supports K-fiber shrinkage, inhibits EB1 binding, and biases individual kMT plus ends toward the shrinking (curved) conformation. Correlative video LM and electron tomography studies will be required to test this model.

Although taxol treatment stabilizes MTs and enhances the straight conformation in kMTs, taxol also inhibits both oscillations and incorporation of tubulin subunits into kMT plus ends [20]. This means that in taxol-treated cells, the K-fibers, and presumably most of the individual kMTs, are in the paused state [34–36]. The paused state is an established feature of MTdynamics, but to our knowledge, the plus-end conformation of MTs in the paused state has not been reported. Our results with taxol-treated cells indicate that kMTs in the paused state can adopt the straight conformation (Figure 2). Because taxol also reduces tension across the kinetochore, it is tempting to speculate that tension arises from the kinetochore preventing curved conformations from disassembling [20,37]. However, we did not expose the cells to taxol long enough to significantly reduce tension, and our measurements of the distance between sister kinetochores in EM serial sections confirmed that tension in the taxol-treated data set was equivalent to that in control metaphase cells (data not shown). Hence, it appears that kMTs with the straight plus-end conformation can also generate tension.

The model proposed in Figure 5 bears a striking resemblance to the release-capture model proposed by Zhai et al. to explain kMT turnover in $PtK_1$ cells [30]. A similar model was recently evoked to explain how kinetochores remain stably attached during mitosis in *Drosophila* embryos, despite a relatively high kMT turn-over rate [38]. The critical new feature in our model is that the dynamic instability cycle can take place on the surface of the outer plate without kMTs being released. Hence, kMT catastrophe rate is not necessarily predictive of kMT release rate. Another key feature of the model in Figure 5 is that attachment to the outer plate prevents kMT plus ends in the curved conformation from disassembling, unless disassembly is coupled to kinetochore movement. This feature explains why kMTs are relatively stable against disassembly conditions such as cold, drug, or calcium treatments. Our model and the release-capture model are not mutually exclusive. Rather, we envision the dynamic instability cycles proposed by the two models taking place simultaneously. The relative contribution of each cycle to kMT dynamics depends upon the

kMT release rate. The kMT release rate appears to be a regulated parameter because kMT turnover can vary considerably with: temperature, stage of mitosis (in $PtK_1$ cells, turnover is much slower during anaphase), and species and/or tissue (in *Drosophila* embryos, turnover is relatively rapid) [30,39]. Thus, the outer plate cycle of our model is expected to be a more dominant factor in kMT dynamics in systems in which the kMT release rate is low (e.g., $PtK_1$ cells) than in systems in which kMT turnover is high (e.g., *Drosophila* embryos).

An alternative model to the one presented in Figure 5 is that under tension and the local environment of the kinetochore, tubulin assembles onto kMT plus ends in the curved conformation. Although we cannot currently rule out this mechanism, we find it less attractive because the curved end conformation is indicative of a GDP-tubulin lattice and there is no precedent for the straight MT lattice forming from the GDP tubulin [13,40]. Rather, a considerable amount of energy appears to be released from the disassembly of straight MTs in which the GTP-tubulin has hydrolyzed to GDP-tubulin [41]. In contrast, the model in Figure 5 is built upon processes that are known to occur including cycles of dynamic instability and stable kinetochore attachment to the plus ends of disassembling MTs.

In summary, our data indicate the existence of a novel mechanism for coordination of MT dynamics and kinetochore function, in which attachment to the outer plate prevents depolymerization of kMT plus ends. Factors controlling kMT dynamics at the kinetochore appear to work by changing the probability that kMTs are in a given dynamic state, rather than by directly controlling the dynamics of individual kMTs. Hence, kinetochores generally show a bias toward one of the two conformations, rather than a tight coordination of their individual kMTs (Figure 3). These data have important ramifications for current attempts to build more comprehensive models of mitosis because all such models require an accurate description of kMT dynamics [32,38,42]. Our simple model implies that the outer plate mediates control mechanisms that bias kMT dynamics. Therefore, it is critical to understand the molecular architecture of the outer plate and how this structure interacts with other molecular components to mediate both the dynamics and the attachment of kMTs. This endeavor requires the synthesis of structural and molecular approaches, and we are currently engaged in such efforts.

## Supplementary Material

Refer to Web version on PubMed Central for supplementary material.

## Acknowledgments

We dedicate this paper to the memory of Rita M. Barnard who performed much of the initial work of this project but was tragically unable to see its completion. We wish to thank Thomas Portuese, Alex Leahey, David Smith, and Wenji Zhang for help with various stages of the computation and analysis and Chyong Ere Hsieh for initial help with high-pressure freezing, freeze substitution, and electron microscopy. We also thank Drs. Alexey Khodjakov, Michael Koonce, and Conly Reider for helpful discussions. This work was supported by National Institutes of Health R01 GM06627 and National Science Foundation MCB 0110821 to B.F.M. We also acknowledge National Institutes of Health P41 RR01219 and National Science Foundation DBI9871347 to Joachim Frank to support the Wadsworth Center's Resource for Biological Complexity and the FEI Tecnai F20 electron microscope. H.M. was supported by POCI/SAU-MMO/58353/2004 (to H.M.) and National Institutes of Health R01 GM40198 to Conly Rieder. Finally, we are grateful for technical support from the Wadsworth Center's Core Facility for Electron Microscopy.

## References

1. Rieder CL, Salmon ED. The vertebrate cell kinetochore and its roles during mitosis. Trends Cell Biol 1998;8:310–318. [PubMed: 9704407]

2. Maiato H, Deluca J, Salmon ED, Earnshaw WC. The dynamic kinetochore-microtubule interface. J Cell Sci 2004;117:5461–5477. [PubMed: 15509863]

3. McEwen BF, Heagle AB, Cassels GO, Buttle KF, Rieder CL. Kinetochore fiber maturation in PtK1 cells and its implications for the mechanisms of chromosome congression and anaphase onset. J Cell Biol 1997;137:1567–1580. [PubMed: 9199171]

4. McIntosh JR, Grishchuk EL, West RR. Chromosome-microtubule interactions during mitosis. Annu Rev Cell Dev Biol 2002;18:193–219. [PubMed: 12142285]

5. Kline-Smith SL, Walczak CE. Mitotic spindle assembly and chromosome segregation: refocusing on microtubule dynamics. Mol Cell 2004;15:317–327. [PubMed: 15304213]

6. Mitchison T, Evans L, Schulze E, Kirschner M. Sites of microtubule assembly and disassembly in the mitotic spindle. Cell 1986;45:515–527. [PubMed: 3708686]

7. Gorbsky GJ, Sammak PJ, Borisy GG. Microtubule dynamics and chromosome motion visualized in living anaphase cells. J Cell Biol 1988;106:1185–1192. [PubMed: 3283149]

8. Mitchison TJ, Salmon ED. Poleward kinetochore fiber movement occurs during both metaphase and anaphase-A in newt lung cell mitosis. J Cell Biol 1992;119:569–582. [PubMed: 1400593]

9. Mandelkow EM, Mandelkow E, Milligan RA. Microtubule dynamics and microtubule caps: a time-resolved cryo-electron microscopy study. J Cell Biol 1991;114:977–991. [PubMed: 1874792]

10. Chretien D, Fuller SD, Karsenti E. Structure of growing microtubule ends: two-dimensional sheets close into tubes at variable rates. J Cell Biol 1995;129:1311–1328. [PubMed: 7775577]

11. Arnal I, Karsenti E, Hyman AA. Structural transitions at microtubule ends correlate with their dynamic properties in *Xenopus* egg extracts. J Cell Biol 2000;149:767–774. [PubMed: 10811818]

12. Janosi IM, Chretien D, Flyvbjerg H. Structural microtubule cap: stability, catastrophe, rescue, and third state. Biophys J 2002;83:1317–1330. [PubMed: 12202357]

13. Wang HW, Nogales E. Nucleotide-dependent bending flexibility of tubulin regulates microtubule assembly. Nature 2005;435:911–915. [PubMed: 15959508]

14. McEwen BF, Marko M. The emergence of electron tomography as an important tool for investigating cellular ultra-structure. J Histochem Cytochem 2001;49:553–564. [PubMed: 11304793]

15. McIntosh R, Nicastro D, Mastronarde D. New views of cells in 3D: an introduction to electron tomography. Trends Cell Biol 2005;15:43–51. [PubMed: 15653077]

16. Lucic V, Foster F, Baumeister W. Structural studies by electron tomography: from cells to molecules. Annu Rev Biochem 2005;74:833–865. [PubMed: 15952904]

17. O'Toole ET, McDonald KL, Mantler J, McIntosh JR, Hyman AA, Muller-Reichert T. Morphologically distinct microtubule ends in the mitotic centrosome of *Caenorhabditis elegans*. J Cell Biol 2003;163:451–456. [PubMed: 14610052]

18. Jordan MA, Wilson L. The use and action of drugs in analyzing mitosis. Methods Cell Biol 1999;61:267–295. [PubMed: 9891320]

19. Skibbens RV, Skeen VP, Salmon ED. Directional instability of kinetochore mobility during chromosome congression and segregation in mitotic newt lung cells: a push-pull mechanism. J Cell Biol 1993;122:859–875. [PubMed: 8349735]

20. Waters J, Mitchison TJ, Rieder CL, Salmon ED. The kinetochore microtubule minus-end disassembly associated with poleward flux produces a force that can do work. Mol Biol Cell 1996;7:1547–1558. [PubMed: 8898361]

21. Maiato H, Khodjakov A, Rieder CL. Drosophila CLASP is required for the incorporation of microtubule subunits into fluxing kinetochore fibres. Nat Cell Biol 2005;7:42–47. [PubMed: 15592460]

22. Salmon ED. Pressure-induced depolymerization of spindle microtubules. I. Changes in birefringence and spindle length. J Cell Biol 1975;65:603–614. [PubMed: 1133117]

23. Mitchison, T. Chromosome alignment at mitotic metaphase: balanced forces or smart kinetochores?. In: Warner, FD.; McIntosh, JR., editors. Kinesin, Dynein, and Microtubule Dynamics. Vol. 2. New York: Alan R. Liss, Inc; 1989. p. 421-430.

24. Wadsworth P, Shelden E, Rupp G, Rieder CL. Biotin-tubulin incorporates into kinetochore fiber microtubules during early but not late anaphase. J Cell Biol 1989;109:2257–2265. [PubMed: 2681228]
25. Ohi R, Coughlin ML, Lane WS, Mitchison TJ. An inner centromere protein that stimulates the microtubule depolymerizing activity of a KinI kinesin. Dev Cell 2003;5:309–321. [PubMed: 12919681]
26. Kline-Smith SL, Khodjakov A, Hergert P, Walczak CE. Depletion of centromeric MCAK leads to chromosome congression and segregation defects due to improper kinetochore attachments. Mol Biol Cell 2004;15:1146–1159. [PubMed: 14699064]
27. McEwen BF, Heagle AB. Electron microscopy tomography: a tool for probing the structure and function of sub-cellular components. J Imaging Syst Tech 1997;8:175–187.
28. McEwen BF, Hsieh CE, Mattheyses AL, Rieder CL. A new look at kinetochore structure in vertebrate somatic cells using high-pressure freezing and freeze substitution. Chromosoma 1998;107:366–375. [PubMed: 9914368]
29. Cassimeris L, Rieder CL, Rupp G, Salmon ED. Stability of microtubule attachment to metaphase kinetochores in PtK1 cells. J Cell Sci 1990;96:9–15. [PubMed: 2197288]
30. Zhai Y, Kronebusch PJ, Borisy GG. Kinetochore microtubule dynamics and the metaphase-anaphase transition. J Cell Biol 1995;131:721–734. [PubMed: 7593192]
31. Nicklas RB. How cells get the right chromosomes. Science 1997;275:632–637. [PubMed: 9005842]
32. Gardner MK, Pearson CG, Sprague BL, Zarzar TR, Bloom K, Salmon ED, Odde DJ. Tension-dependent regulation of microtubule dynamics at kinetochores can explain metaphase congression in yeast. Mol Biol Cell 2005;16:3764–3775. [PubMed: 15930123]
33. Tirnauer JS, Canman JC, Salmon ED, Mitchison TJ. EB1 targets to kinetochores with attached, polymerizing microtubules. Mol Biol Cell 2002;13:4308–4316. [PubMed: 12475954]
34. Shelden E, Wadsworth P. Observation and quantification of individual microtubule behavior in vivo: microtubule dynamics are cell-type specific. J Cell Biol 1993;120:935–945. [PubMed: 8432733]
35. Khodjakov A, Rieder CL. Kinetochores moving away from their associated pole do not exert a significant pushing force on the chromosome. J Cell Biol 1996;135:315–327. [PubMed: 8896591]
36. Rusan NM, Fagerstrom CJ, Yvon AM, Wadsworth P. Cell cycle-dependent changes in microtubule dynamics in living cells expressing green fluorescent protein-alpha tubulin. Mol Biol Cell 2001;12:971–980. [PubMed: 11294900]
37. Waters J, Chen RH, Murray AW, Salmon ED. Localization of Mad2 to kinetochores depends on microtubule attachment, not tension. J Cell Biol 1998;141:1181–1191. [PubMed: 9606210]
38. Civelekoglu-Scholey G, Sharp DJ, Mogilner A, Scholey JM. Model of chromosome motility in *Drosophila* embryos: adaptation of a general mechanism for rapid mitosis. Biophys J 2006;90:3966–3982. [PubMed: 16533843]
39. Brust-Mascher I, Civelekoglu-Scholey G, Kwon M, Mogilner A, Scholey JM. Model for anaphase B: role of three mitotic motors in a switch from poleward flux to spindle elongation. Proc Natl Acad Sci USA 2004;101:15938–15943. [PubMed: 15522967]
40. Muller-Reichert T, Chretien D, Severin F, Hyman AA. Structural changes at microtubule ends accompanying GTP hydrolysis: information from a slowly hydrolyzable analogue of GTP, guanylyl (alpha, beta)methylenediphosphonate. Proc Natl Acad Sci USA 1998;95:3661–3666. [PubMed: 9520422]
41. Grishchuk EL, Molodtsov MI, Ataullakhanov FI, Mc-Intosh JR. Force production by disassembling microtubules. Nature 2005;438:384–388. [PubMed: 16292315]
42. Mogilner A, Wollman R, Civelekoglu-Scholey G, Scholey J. Modeling mitosis. Trends Cell Biol 2006;16:88–96. [PubMed: 16406522]

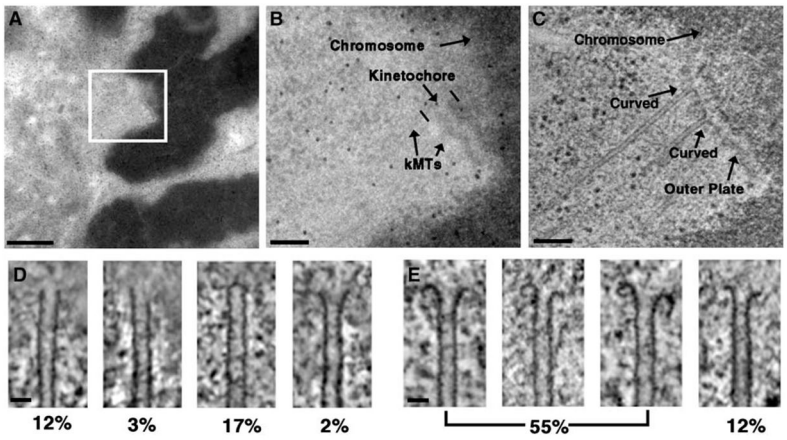


**Figure 1.**

Illustration of the Use of Electron Tomography to Identify the Plus-End Conformations of kMTs in $PtK_1$ Cells

(A) EM image of a 200 nm thick plastic section containing a metaphase chromosome from a $PtK_1$ cell prepared by high-pressure freezing and freeze substitution. Scale bar = 1 μm.

(B) Higher magnification image of the boxed area in (A), with the chromosome, kinetochore, and kMTs labeled. Scale bar = 200 nm.

(C) A 1.6 nm thick slice from the tomographic reconstruction of the same area represented in (B). The kinetochore outer plate and two kMTs displaying the curved conformation are indicated. Scale bar = 200 nm.

(D and E) Examples of the range of straight (D) and curved (E) conformations that were detected for the plus ends of kMTs by electron tomography. Underneath each image is the percentage of kMT plus ends in untreated metaphase $PtK_1$ cells having a similar conformation. Scale bars represent 25 nm.

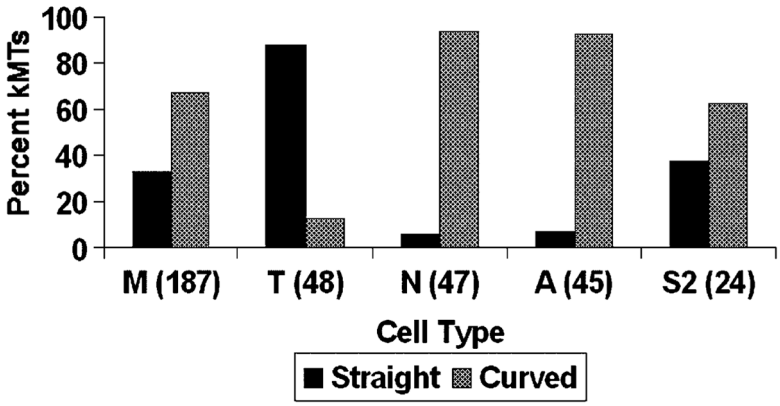


**Figure 2.**

Bar Graph of kMT Plus-End Conformations

The percentage of kMT plus ends classified as straight and curved are plotted for: M, untreated metaphase; T, taxol-treated metaphase; N, nocodazole-treated metaphase; A, untreated anaphase $PtK_1$ cells; and S2, untreated metaphase *Drosophila* S2 cells. The sample size (number of kMT plus ends classified) is indicated in parentheses on the abscissa.

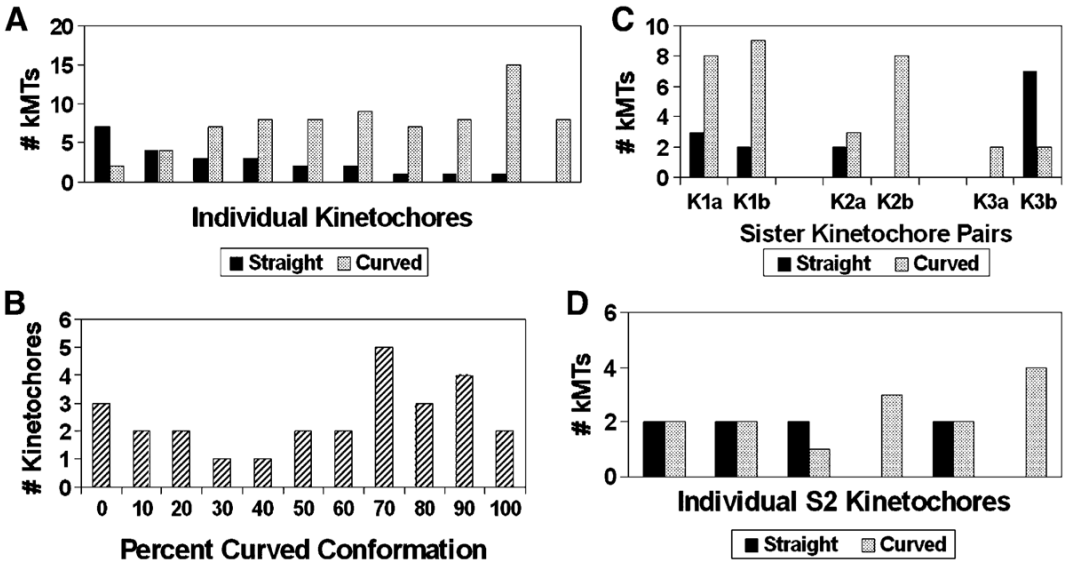


**Figure 3.**

Plus-End Conformations of the kMTs in Individual K-Fibers from Metaphase $PtK_1$ and S2 Cells

(A) A plot of the number of kMT plus ends classified in the straight and curved conformations for ten K-fibers from four different cells. On average, K-fibers in $PtK_1$ cells contain 23 MTs [3], but for technical reasons, we only analyzed 8–16 plus ends per kinetochore as a random sampling of the total. The ordering of kinetochores along the abscissa is by increasing percentage of kMTs found in the curved conformation.

(B) Histogram of the percentage of kMTs exhibiting the curved conformation in 27 K-fibers, for which 3–16 kMTs each were analyzed. The broad distribution with a weak secondary peak at a low percentage of curved plus ends indicates that the kMT plus-end conformations within a given K-fiber are not completely random.

(C) A plot of the number of kMT plus ends classified in the straight and curved conformations for K-fibers from three pairs of sister kinetochores in PTK metaphase cells.

(D) A plot of the number of kMT plus ends classified in the straight and curved conformations for six K-fibers from a S2 cell.

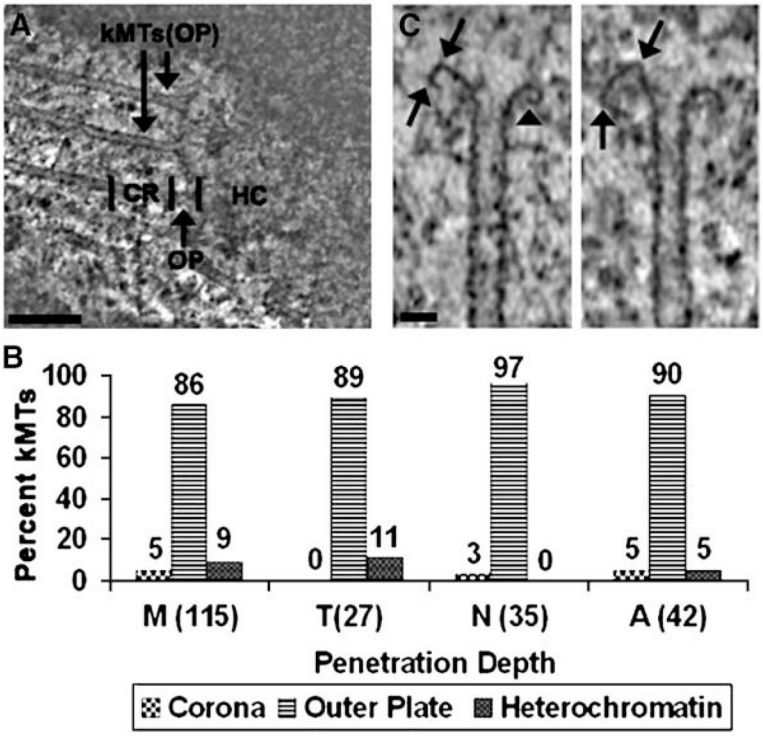


**Figure 4.**

Depth that kMTs Penetrated into the Centromere

(A) A single 10 nm thick slice from a tomographic reconstruction, with regional delineations for the corona (CR), outer plate (OP), and heterochromatin (HC). Two kMTs terminating in the outer plate are indicated (kMTs [OP]). Scale bar = 200 nm.

(B) Bar graph of kMT penetration. The percentages of kMTs terminating in the three regions delineated in (A) are indicated above the bars for: M, untreated; T, taxol treated; N, nocodazole-treated metaphase $PtK_1$ cells; and A, untreated anaphase $PtK_1$ cells. The sample sizes are indicated in parentheses on the abscissa. Measurements were limited to kinetochores for which a clearly defined outer plate was visible.

(C) Curved plus ends showing the kinks (arrows) and tight-radius curvatures (arrowhead) that were frequently observed. Scale bar = 25 nm.

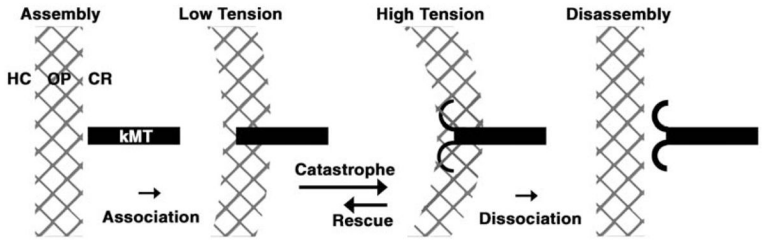


**Figure 5.**

Model for kMT Dynamic Instability on PtK1 and *Drosophila* S2 Kinetochores

A single kMT is shown undergoing a conformational change from straight (left side) to curved (right side). A key feature of the model is that attachment to the outer plate prevents kMT disassembly that is not coupled to chromosome motion. This enables kMTs in the disassembly phase to be rescued, which in turn results in a continual cycling of individual kMTs that are in the growing phase. The cycling of kMTs between the growing and shrinking phases permits net incorporation of tubulin into the plus end of the K-fiber, even though the majority of its kMTs are in the disassembly phase. The catastrophe rate is shown as twice the rescue rate because that generates a 1:2 ratio of straight to curved conformations. Dissociation from the outer plate is low in $PtK_1$ cells but is much higher in cells with a high kMT turnover rate. In the latter case, dynamic cycles of MT growth and shrinkage would occur primarily in the spindle, rather than on the kinetochore outer plate. However, the principle of cycling between which individual kMTs are contributing to K-fiber growth would be the same. The heterochromatin (HC), outer plate (OP), and corona (CR) designations are the same as those given in Figure 4A.